Int. J. Heat Mass Transfer. Vol. 17, pp. 767–783. Pergamon Press 1974. Printed in Great Britain

DYNAMICS OF HEAT TRANSFER FROM CYLINDERS IN A TURBULENT AIR STREAM

MAHER I. BOULOS* and DAVID C. T. PEI
Chemical Engineering Department, University of Waterloo, Waterloo, Ontario, Canada

(*Received* 11 *December* 1972 *in revised form* 8 *November* 1973)

Abstract—An investigation has been carried out to study the dynamics of the transfer of heat from a circular cylinder in a turbulent air stream with emphasis on the wake region.

The results, obtained over a Reynolds number range from 3000 to 9000, clearly indicate that the wake is comprised of two distinct regions; the secondary and the main vortex regions. The former extends between 85 and 130–150° from the front stagnation point, while the latter covers the remaining area of the wake. These two regions are shown to react differently to variations in the free-stream conditions.

NOMENCLATURE

- d, cylinder diameter;
- f, frequency;
- FP, power spectral density function, equation (6);
- h', RMS of the fluctuation in the heat-transfer coefficient;
- $\bar{H}$, time-averaged heat-transfer coefficient;
- k, thermal conductivity;
- L_f, integral scale of turbulence;
- M, lag number;
- N_{Nu}, Nusselt number $[\bar{H}d/k]$;
- N_{Re}, Reynolds number $[Ud\rho/\mu]$;
- $P(v)$, probability density function, equation (3);
- Q_v, autocorrelation function, equation (4);
- RP, autocorrelation coefficient, equation (5);
- $Tu\%$, intensity of turbulence $[100\,u'/\bar{U}]$;
- u', RMS of the velocity fluctuation;
- $\bar{U}$, time-averaged free stream velocity;
- v, bridge voltage;
- x, distance in the direction of flow.

Greek letters

- $\eta\%$, intensity of the fluctuation in the heat-transfer rate $[100\,h'/\bar{H}]$;
- θ, angle from the front stagnation point;
- μ, dynamic viscosity;
- ρ, density;
- τ, time.

List of abbreviations

- CHF, constant heat flux;
- CTA, constant temperature anemometer;
- CWT, constant wall temperature;
- fsp, front stagnation point;
- PDF, probability density function;
- RMS, root mean square;
- rsp, rear stagnation point.

INTRODUCTION

GENERALLY it has been accepted that the overall heat-transfer rate from a circular cylinder may be correlated by separating the boundary-layer and wake contributions to the overall transfer. The correlations proposed by Douglas and Churchill [1] and Richardson [2] are typical examples. These are as follows.

Douglas and Churchill [1]

$$N_{Nu} = 0{\cdot}46\,N_{Re}^{0{\cdot}5} + 0{\cdot}00128\,N_{Re} \tag{1}$$

Richardson [2]

$$N_{Nu} = C_1 N_{Re}^{0{\cdot}5} + C_2 N_{Re}^{0{\cdot}67} \tag{2}$$

where

$$0{\cdot}37 < C_1 < 0{\cdot}55$$

$$0{\cdot}057 < C_2 < 0{\cdot}084.$$

The first term on the r.h.s. of both correlations represents the boundary-layer contribution, while the second term represents the wake contribution to the overall transfer. It is observed that, in contrast to the boundary-layer region, there is a large difference between the Reynolds number exponents used for the wake contribution term. Moreover, Richardson's exponent of 0·67 is based on measurements at the rear stagnation point. It implies that the heat-transfer rate over the wake region has a similar Reynolds number dependence. Such an assumption is at variance with the results of Churchill and Brier [3] who reported an increase in the Reynolds exponent from 0·25 at 90° from the front stagnation point, to about 0·9 at the rear stagnation point.

*Present address: Chemical Engineering Department, University of Sherbrooke, Sherbrooke, Quebec, Canada.

Flow visualization [4, 5] as well as hot wire probing [6, 7] supplies further evidence of the fact that the flow over the wake region has different characteristics around the separation point from the rear stagnation point. For example, it is reported by Bloor [7] that at Reynolds numbers less than 10^4, a laminar shear layer is formed as the boundary layer separates from the surface of the cylinder. Beyond one radius from the separation point, the free shear layer degenerates into turbulence which results in a turbulent flow over the rear stagnation point. Such a difference in the flow conditions over the surface of the cylinder will undoubtedly affect the local heat-transfer rates.

The present investigation is aimed specifically at studying the details of the transport process over the wake region. Since the wake flow pattern is unsteady at Reynolds numbers above 50, it is important to determine the dynamic as well as the time-averaged heat-transfer rate characteristics. This was achieved using standard thin film techniques.

The local heat-transfer rate was measured using a thin platinum film sensor deposited on a small surface area of the cylinder and heated by a constant temperature anemometer unit. The linearized bridge voltage, which is proportional to the instantaneous rate of heat dissipation from the sensor, was used to calculate the local time-average heat-transfer coefficient and the intensity of heat transfer rate fluctuations. The latter parameter is defined as the ratio of the RMS of the fluctuations in the heat-transfer rate to its mean value.

In order to provide the necessary temperature history of the thermal boundary layer and to reduce heat conduction to the backing material, the main body of the cylinder was separately heated. The constant heat flux and the constant wall temperature cases have been investigated.

HEAT-TRANSFER RATE MEASUREMENTS UNDER CONSTANT HEAT FLUX CONDITIONS

Experimental technique

The cylinder used for the local and overall heat-transfer rate measurements under CHF (constant heat flux) conditions is shown in Fig. 1. It was made of a Vycor tube (1·87 cm O.D. and 17·5 cm long) with four thin platinum film sensors deposited on its surface.

The local sensor (0·11 cm wide and 1·39 cm long) was oriented parallel to the axis of the cylinder. Its azimuthal span was about 7°.

The overall sensor was 7·5 cm long and covered the remaining central region of the cylinder, but it was electrically insulated from the local sensor. At each end of this sensor, a thin layer of soft solder was applied around the cylinder forming a narrow ring of very small resistance compared to the film resistance. This ensured a uniform current density in the film. The electrical contacts from this film were taken from each of the solder rings by copper wires through the wall of the cylinder.

The other two sensors, which were of a similar construction as the overall sensor, were located on each end of the cylinder. These were used as guard heaters to eliminate axial heat conduction from the central region of the cylinder.

In order to check the local temperature distribution around the cylinder, three other film sensors (0·13 cm wide and 0·76 cm long) were deposited on the inside surface of the cylinder. These were oriented parallel to the axis of the cylinder with one of them underneath the local sensor and one on each side of it.

Due to the presence of temperature gradients around the cylinder, special precautions were taken to minimize internal heat transfer within the cylinder. The cylinder used had a wall which is 0·13 cm thick. It was con-

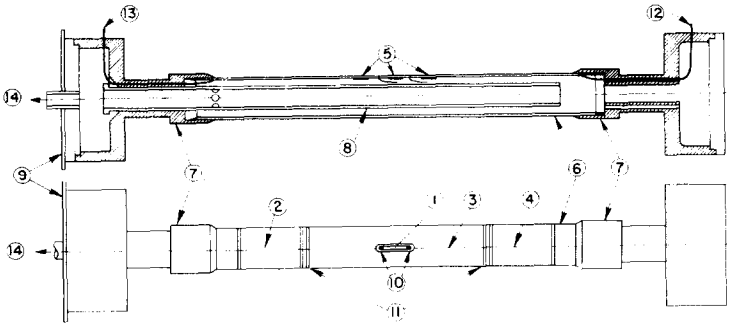

FIG. 1. Constant heat flux test cylinder.

sidered to be the minimum thickness for reasonable mechanical strength. The cylinder was evacuated to within 0·01 mm mercury, and an internal radiation shield was installed. This was a highly-polished, chromeplated, thin wall brass tube (1·14 cm O.D.) located centrally inside the test cylinder.

After the construction of the cylinder, all the sensors were calibrated to within $\pm 0{\cdot}2°C$. The frequency response of the local sensor was measured by the indirect method of Nielsen and Rasmussen [8]. Its -3dB point was around 100 Hz. At higher frequencies, the attenuation gradually increased until it reached the characteristic drop of -10dB/decade around 1 KHz.

Such a frequency response might seem rather low for significant dynamic measurements. However, over the Reynolds number range investigated, the fundamental shedding frequency ranged between 30 and 110 Hz, and thus was little attenuated. Over the higher frequency end of the spectrum, the measured fluctuations in the heat-transfer rate will obviously be attenuated. The effect, being common to all measurements, will not affect their relative values.

Experiments were carried out in the test section (20×20 cm) of a low speed, closed loop, wind tunnel. The cylinder was mounted over two brackets which allowed it to be rotated about its axis. The angle between the local sensor and the front stagnation point was measured using a vernier protractor. The intensity and scale of turbulence at the position of the cylinder, could be varied over the ranges from 1 to 6 per cent and from 0·2 to 0·8 cm respectively. This was achieved using turbulence-generating grids at the entrance of the test section and by changing the distance between the grid and the centerline of the cylinder. Details of the construction and calibration of the wind tunnel can be found elsewhere [9].

Data acquisition

A block diagram of the circuit used is shown in Fig. 2.

The local sensor was heated using the high sensitivity bridge of a TSI 1010A CTA (constant temperature anemometer) unit. The overall sensor and one of the guard heaters were operated using the high power bridges of two CTA units, while the second guard heater was operated by a manually controlled bridge. The temperature (operating resistance) of the local sensor was adjusted such that the heat flux per unit area of the local sensor was equal to that dissipated by the overall sensor.

Measurements were made of the operating resistance of all sensors, the temperature of the resistance thermometers on the inside surface of the cylinder and the pertinent anemometer bridge voltages. The a.c. component of the signal from the local sensor was recorded by a Hewlett Packard 3914B FM magnetic tape recorder for later dynamic analysis.

The time-averaged local and overall heat-transfer coefficients were calculated from the sensor current, its operating resistance and its average surface temperature. The corresponding Nusselt number was obtained with the air property values evaluated at the mean film temperature.

The intensity of the local heat-transfer rate fluctuations, η, was calculated from the ratio of the RMS (root mean square) of the linearized bridge voltage to its d.c. component.

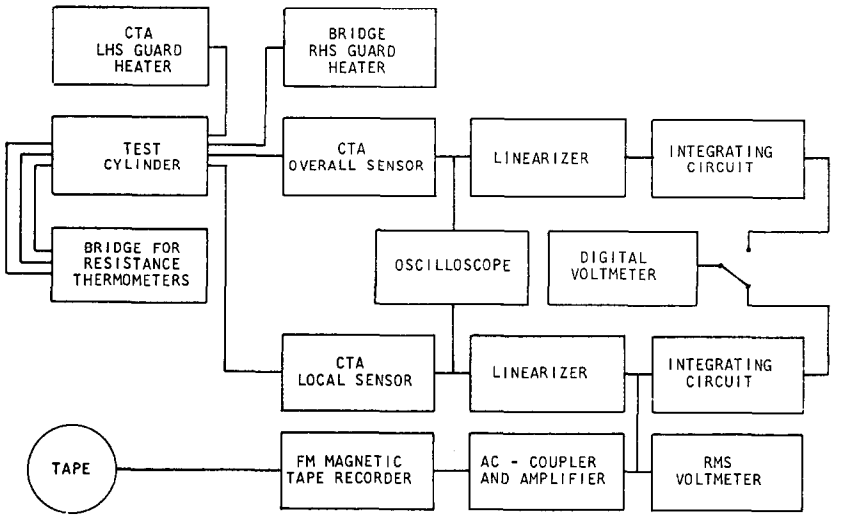

FIG. 2. Block diagram of the circuit used for the local and overall heat-transfer rate measurements under CHF conditions.

The bridge voltage fluctuations, stored on magnetic tape, were subjected to a number of statistical data analysis. The analogue signal was first converted into a digital record of 60000 data points obtained at a sampling rate of 2000 samples per second. After detrending and normalizing the data, the following statistical functions were calculated on an IBM 360-44 computer.

(a) *Probability density function.* It is defined as the probability that the signal will assume a value within some definite range at any instant

$$P(v) = \lim_{\Delta v \to 0} \frac{\text{Prob}(v < v(\tau) < v + \Delta v)}{\Delta v}. \quad (3)$$

(b) *Autocorrelation function.* It is defined as

$$Q_v(j\Delta\tau) = \frac{1}{(N-j)\Delta\tau} \sum_{i=0}^{(N-j)} v[i\Delta\tau]v[(i+j)\Delta\tau]\Delta\tau \quad (4)$$

where j is the lag number $j = 0, 1, \ldots, M$.

When normalized we obtain the autocorrelation coefficient

$$RP(j\Delta\tau) = \frac{Q_v(j\Delta\tau)}{Q_v(0)}. \quad (5)$$

(c) *Power spectral density function.* It was obtained by calculating the Fourier transform of the autocorrelation coefficient

$$FP(f) = 4\Delta\tau\left[0{\cdot}5RP(0) + \sum_{j=1}^{M-1} RP(j\Delta\tau)\cos(2\pi fj\Delta\tau) + 0{\cdot}5RP(M\Delta\tau)\cos(2\pi fM\Delta\tau)\right]. \quad (6)$$

Evaluation of the experimental technique

The accuracy of the data obtained depends on the three major factors.

(a) *Characteristics of the constant temperature anemometer bridge.* When considering the accuracy of the time-averaged heat-transfer rate measurements, the most important feature of the performance of the CTA bridge is the accuracy by which the bridge is maintained balanced. In other words, how accurately is the sensor maintained at a constant temperature? Since the bridge showed a distinct unbalance voltage for a resistance change of the order of 0·01 Ω, the resistance of the sensor will be constant within such limits. This would correspond to an uncertainty in the temperature measurements of 0·25°C.

(b) *Accuracy of the "read out" instruments.* The instruments used were of good quality and their performance was repeatedly checked during the course of the experiments. Their accuracy will, therefore, be assumed to be within their specifications limits. Based on such accuracy limits, the local time-averaged heat-transfer rate measurements will have a maximum error of about 2·5 per cent. The parameter which contributes most to such an error is the area of the local sensor. Although the dimensions of the local sensor were measured to within 0·001 in. the particularly small size of the sensor limited the area measurement to within 2·3 per cent.

(c) *Assumptions made in the calculation procedure.* The following assumptions were made.

1. *Uniform heat generation around the cylinder*—This implies a uniform film thickness of the overall sensor around the cylinder and negligible changes in its resistivity.

The uniform film thickness assumption is justifiable on the basis of the many precautions taken during the sensor preparation. However, due to the relatively high temperature coefficient of resistance of the sensor material, the local heat generation per unit area of the overall sensor will vary around the cylinder. For the sensor used, the variation will be less than 7 per cent of the average heat flux for a 30°C temperature difference over the surface of the cylinder. Such a change in the local heat flux is almost two orders of magnitude smaller than that observed under CWT conditions. Its effect on the local heat-transfer rate measurements will, therefore, be negligible.

2. *Negligible heat conduction through the backing material*—Internal heat transfer within the cylinder was reduced by evacuating the inner space of the cylinder and the installation of an internal radiation shield. Conduction along the periphery of the cylinder was reduced using a thin wall cylinder.

3. *Negligible heat transfer by radiation*—Due to the highly polished surface of the cylinder and the small temperature difference between the cylinder and its surrounding (about 50°C) radiation contribution to the overall transfer was negligible.

4. *Negligible wind tunnel blockage*—Wind tunnel blockage was about 9·2 per cent. Its effect on the heat transfer rate at the rear stagnation point was estimated to be less than 2 per cent.

RESULTS AND DISCUSSION

Overall heat transfer

Figure 3 shows that, in agreement with earlier literature data, the overall heat-transfer rate increases with the increase in the Reynolds number and the free stream level of turbulence. The effect of free-stream turbulence is slightly more pronounced at higher Reynolds numbers than at lower values. The effect of the integral scale of turbulence was negligible over the range of the present investigation ($0{\cdot}1 < L_f/d < 0{\cdot}4$).

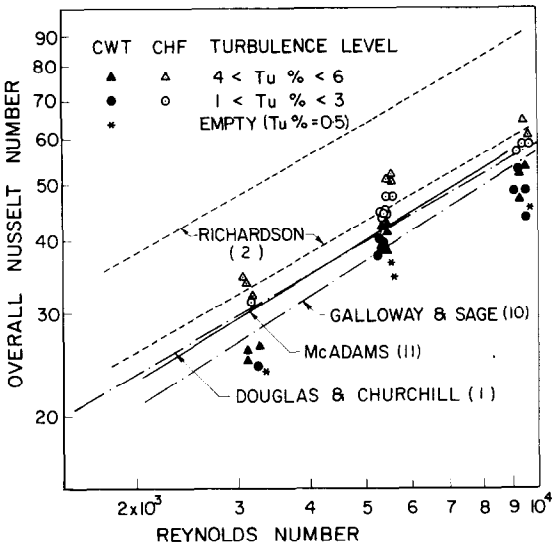

FIG. 3. Variation of the overall Nusselt number with the Reynolds number.

Local time-averaged heat transfer

Local heat-transfer rates over the surface of the cylinder were measured at three nominal Reynolds numbers and different free-stream conditions. Typical distributions are shown in Fig. 4. The complete tabulated data can be found in [9].

It is observed that the local Nusselt number distributions has a minimum around 110° from the front stagnation point. Although the apparant flattening of the distributions could be partially caused by heat conduction along the wall of the cylinder, the location of the minimum heat-transfer rate is characteristic of the transfer under CHF conditions. It has been reported earlier by Matsui *et al.* [12], Dyban and Epick [13]. Mujumdar [14], and Perkins and Leppert [15], over the same Reynolds number range.

The upper part of Fig. 4 shows that the intensity of the fluctuations in the heat-transfer rate is an order of magnitude higher over the wake region than over the boundary-layer region. Around the separation point, 85°, there is consistently a local maximum in the value of η. As will be shown later, spectrum analysis of the signal indicates that the separation point continuously oscillates over this region, at the shedding frequency. Within the wake region, the intensity of heat-transfer rate fluctuations increases steadily with angle until it reaches a maximum at the rear stagnation point.

Figure 5 shows the variation of the local Nusselt number with the Reynolds number over different regions around the cylinder. As expected the Reynolds number has a more pronounced effect on the transfer at the rsp than over the boundary-layer region. However, it is interesting to note that there is a difference between the Reynolds number exponents for the transfer at 120 and 180°.

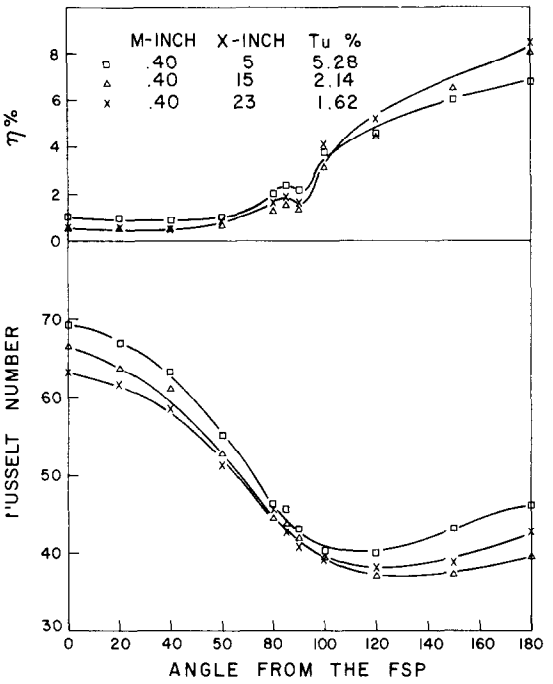

FIG. 4. Local heat-transfer rate distribution under CHF conditions, $N_{Re} = 5400$.

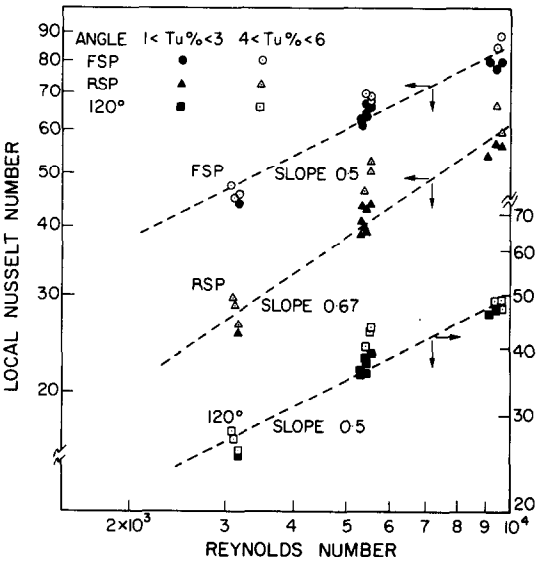

FIG. 5. Variation of the local Nusselt number with the Reynolds number under CHF conditions.

Effect of free-stream turbulence

The present investigation showed that variations of the free-stream intensity of turbulence influenced the local heat-transfer rate in different ways depending on the flow field over the surface of the cylinder. The effect will be evaluated for each region separately.

(a) *Boundary-layer region* ($0° < \theta < 85°$). As shown in Fig. 4, increasing the free-stream intensity of turbulence increases the local heat-transfer rate over the boundary-layer region. The effect is more pronounced at the fsp than around the separation point. It is interesting to note from Figs. 6 and 7 that the increase in heat transfer is accompanied with a corresponding increase in the intensity of the heat-transfer rate fluctuations. Obviously this supports the view that the effect is the result of the penetration of boundary layer by free-stream vortices which increases the "apparent level of turbulence" within the laminar boundary layer.

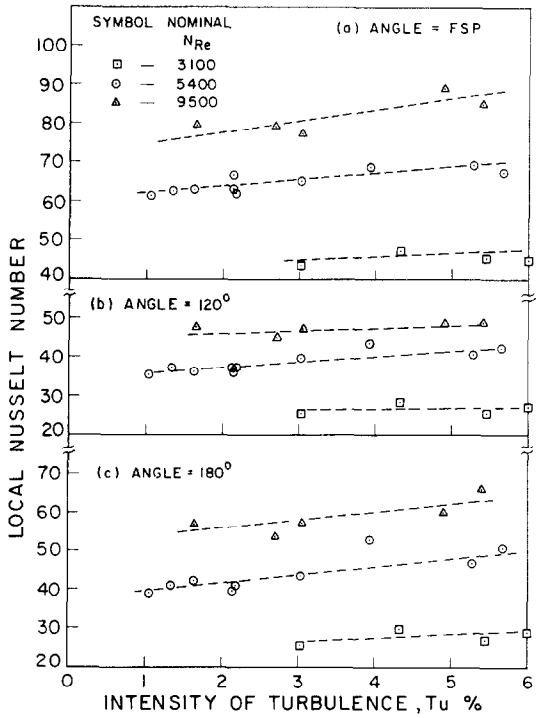

FIG. 6. Effect of free-stream turbulence on the local heat-transfer rate under CHF conditions.

(b) *Wake region* ($85° < \theta < 180°$). While it has long been acceptable to speak of the transfer around a circular cylinder or a sphere in terms of the boundary layer and wake transfer, it seems, in the light of the present investigation, unjustifiable to put all the transfer beyond the separation point into one category. As will be shown later, the wake region actually consists of two distinct flow regions, namely, the secondary and the main vortex regions. The former extends between 85 and 130–150° from the fsp, while the latter covers the remaining area of the wake. It is astonishing that, although the presence of such regions has been earlier recognized from flow visualization experiments [4, 5], they have not been treated as regions of possibly different heat-transfer characteristics.

Secondary vortex region ($85° < \theta < 130$–$150°$)

This region is bounded by the separation point on one side and the main vortex on the other. It is composed of small secondary vortices which, after a certain residence time, are either entrained by the free shear layer or coalesce with the main vortex behind the cylinder. Their residence time does not seem to be directly related to the shedding frequency. However, the boundaries of this region oscillate over the surface of the cylinder at the shedding frequency.

As shown in Figs. 6 and 7, the local heat-transfer rate over this region is not affected by variations of the free-stream intensity of turbulence.

Main vortex region (130–$150 < \theta < 180°$)

The main vortex region of the cylinder is the surface which is in contact with the main vortex during the different stages of its growth. According to Gerrard [16], the main vortex, as it emerges from one of the secondary vortex regions, will be small and weak. As its circulation increases, it gradually grows in size until a point is reached when the vortex becomes large enough to entrain fluid of opposite circulation from the other shear layer. This will put an end to its growing stage and the vortex will be convected downstream as it separates from the cylinder. Such a process repeats itself periodically with its frequency given by the Strouhal number which is constant over the Reynolds number range from 10^3 to 10^5 [5], and is independent of the free-stream level of turbulence [17].

Figure 6 shows that increasing the free-stream intensity of turbulence, causes a corresponding increase in the local time-averaged heat-transfer rate at the rsp. The effect is slightly more pronounced at higher Reynolds numbers.

One important feature of the transfer over the main vortex region, is the high intensity of the heat-transfer rate fluctuations. Increasing the Reynolds number, or the free-stream level of turbulence, reduces the intensity of these fluctuations rather drastically. Figure 7 reveals an interesting reversal of the effect of free-stream turbulence on the intensity of heat-transfer rate fluctuations between the boundary layer and the wake regions of the cylinder. It is observed that, while η increases with the increase in the intensity of turbulence at the fsp, it shows little sensitivity to $Tu\%$ around 120°, and decreases with an increase in $Tu\%$ at the rsp.

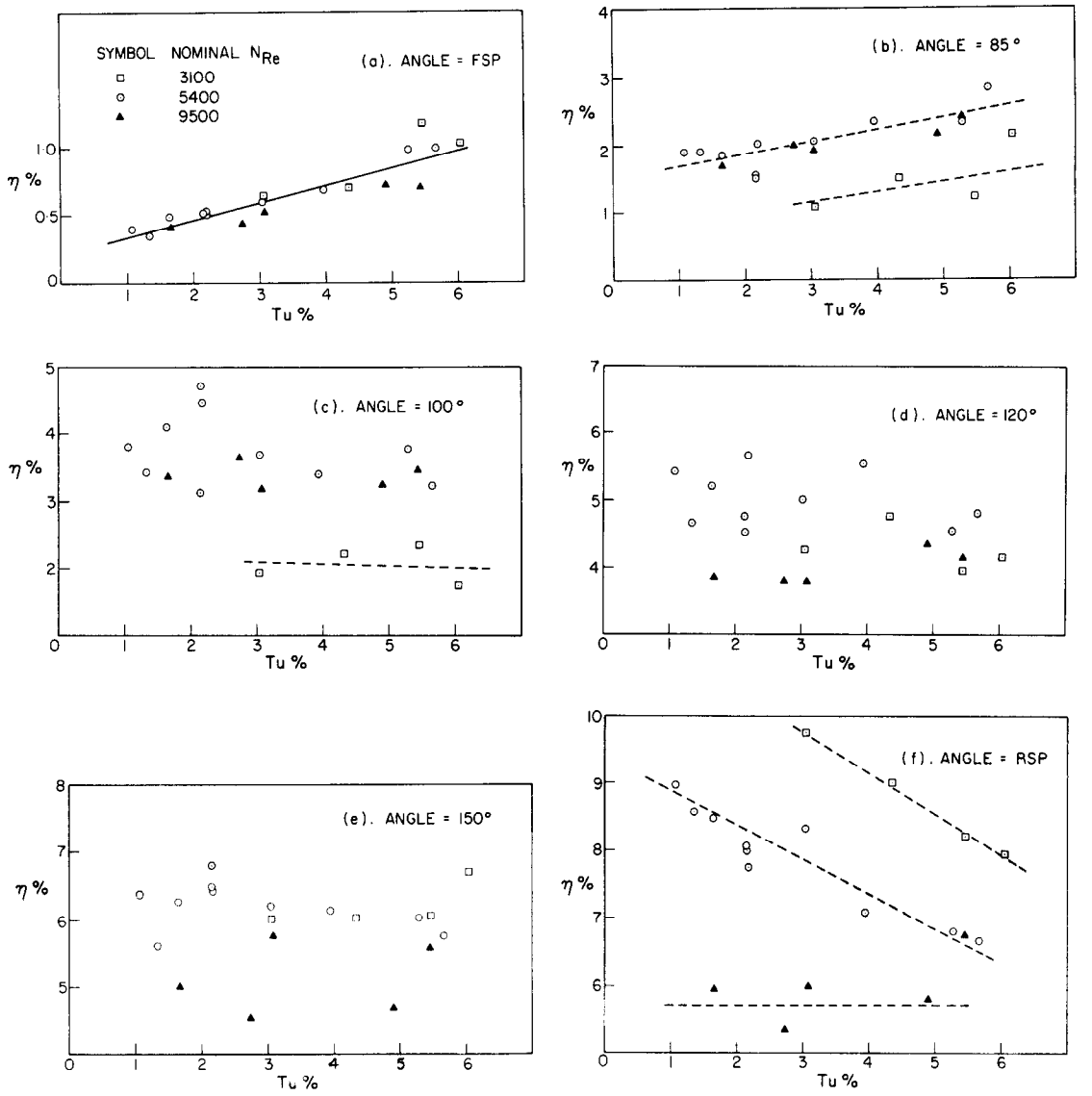

FIG. 7. Effect of free-stream turbulence on the intensity of local heat-transfer rate fluctuations under CHF conditions.

Dynamic aspects of the heat transfer

Typical oscillograms of the linearized bridge voltage fluctuations are shown in Fig. 8.

It is observed that between 80° and 90° from the fsp, there is a pronounced periodicity at the shedding frequency which clearly indicates that the separation point is continuously oscillating over this area. A low frequency oscillation which is an order of magnitude lower than the shedding frequency is also apparent. This is probably caused by three-dimensionality effects which were observed earlier by Gerrard [18] in flows around circular cylinders. Similar low frequency oscillations were also observed in the wake region of a circular cylinder by Hanson and Richardson [6].

Around 100 to 120° from the fsp, the signal becomes more random and is characterized by having pronounced spikes. These could correspond to the sweep of a vortex over the local sensor with its path close enough to the wall of the cylinder.

Between 150 and 180° from the fsp, the signal becomes progressively more random in nature with no detectable signs of periodicity.

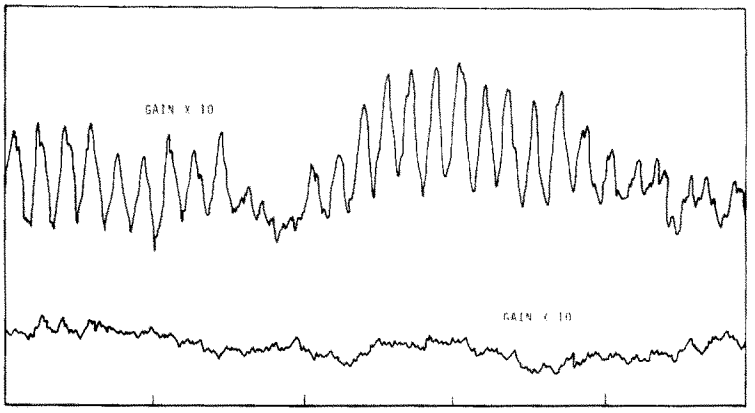

(a) Angle = 80

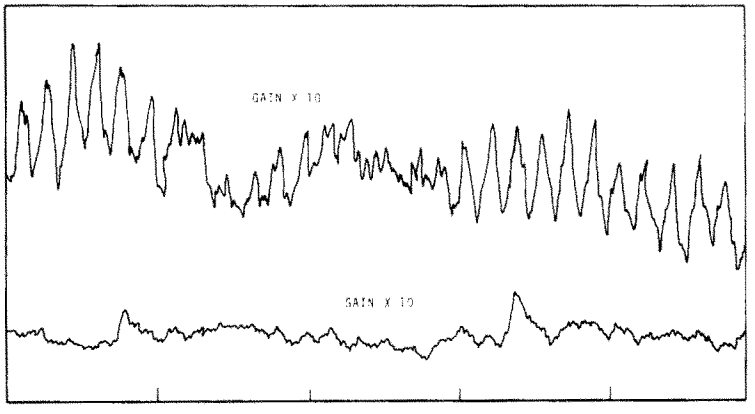

(b) Angle = 90

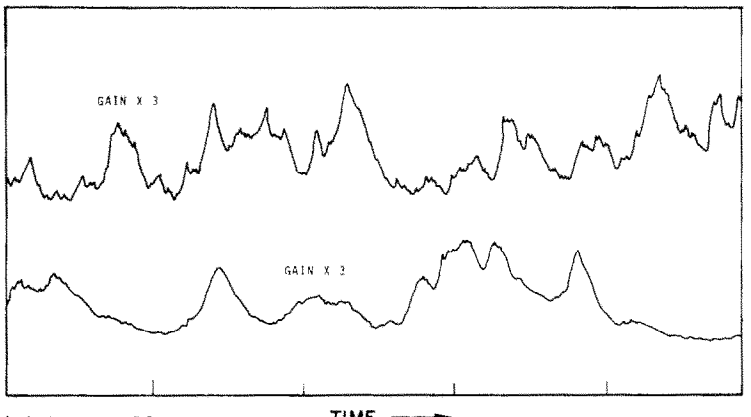

(c) Angle = 100

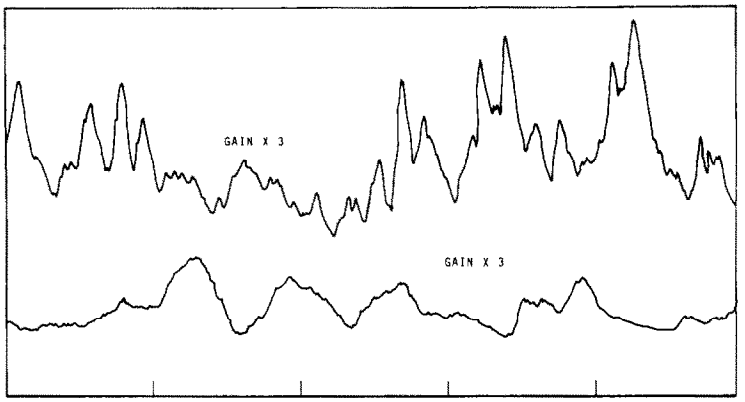

(d) Angle = 120

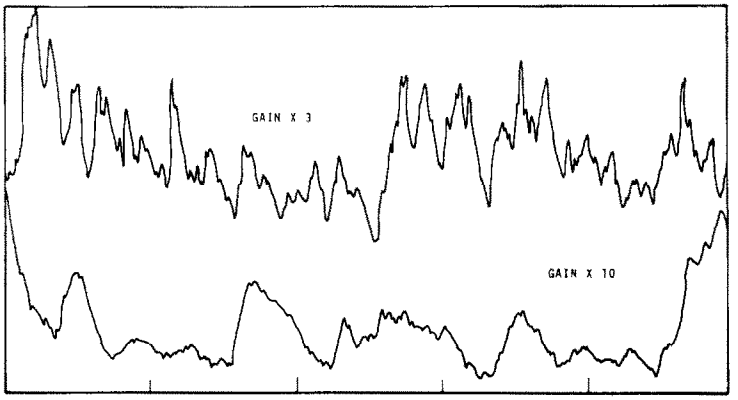

(e) Angle = 150

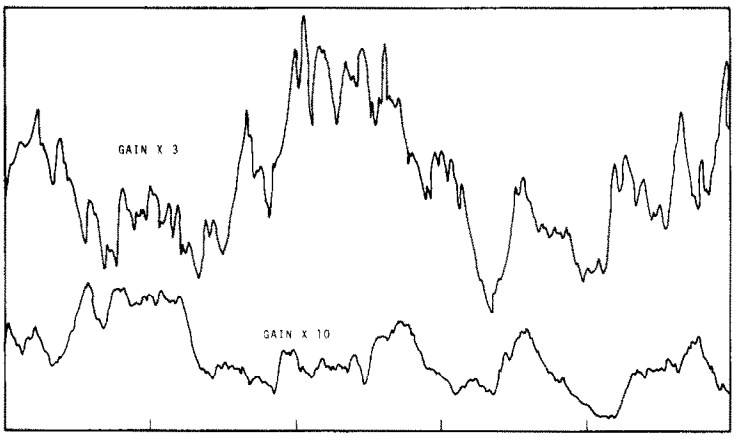

(f) Angle = 180

FIG. 8. Oscillograms of the bridge voltage fluctuations under CHF conditions, TME base = 0·1 s/div.; $N_{Re} = 5400$; $Tu\% = 2{\cdot}14$; lower trace in the presence of a splitter plate at $X/D = 1{\cdot}5$.

The PDF (probability density function) of the fluctuating heat-transfer rate was determined for different angles within the wake region at three nominal Reynolds numbers and different free-stream turbulence conditions. Typical distributions obtained are shown in Fig. 9. A Guassian curve is also plotted in each of these for comparison.

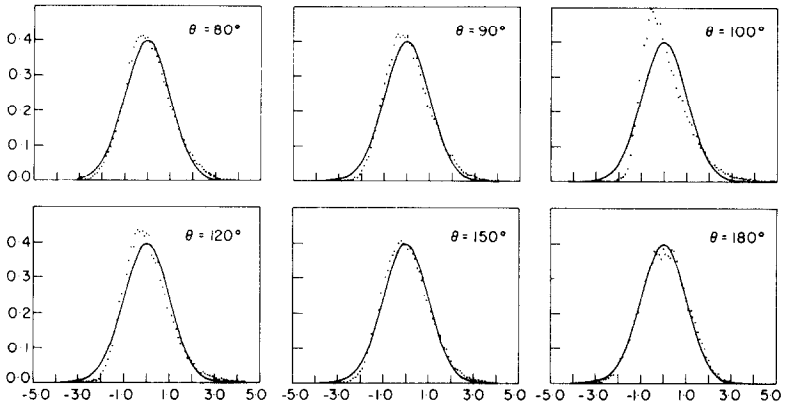

FIG. 9. Probability density function of the heat-transfer rate fluctuations under CHF conditions; $N_{Re} = 5420$; $Tu\% = 2{\cdot}14$.

It is observed that the PDF is essentially normal around the separation point. Between 100 and 120°, it becomes skewed, but shifts back to normality with the increase in the angle beyond 120°. Such a noticeable change in the PDF within the wake region supports the fact that the wake cannot be treated as one big "messy" region, but should be looked upon as possibly two distinct regions.

The above features of the PDF within the wake region were observed consistently under all Reynolds numbers and free-stream turbulence conditions investigated. The respective distribution at any angle was found to be independent of the free-stream conditions.

Further evidence to the existance of two regions within the wake is demonstrated by the results of autocorrelation analysis shown in Fig. 10. The appearance of a distinct periodic component at 150°, while having relatively no periodicity on each side, seems to indicate that the boundary between the secondary and the main vortex regions is oscillating between 120 and 150° at the shedding frequency. In fact, it seems possible to visualize the boundary between these two regions as a point where the strong back flow over the rear surface of the cylinder separates. In other words, it could be considered as the "back flow separation point". Knowing that the boundary-layer separation point oscillates at the shedding frequency, it does not seem unusual to recognize that the "back flow separation point" oscillates also at the shedding frequency. It may be noted that the heat-transfer rate fluctuations at these two locations are affected in a similar fashion by variations in the Reynolds number and the free-stream intensity of turbulence.

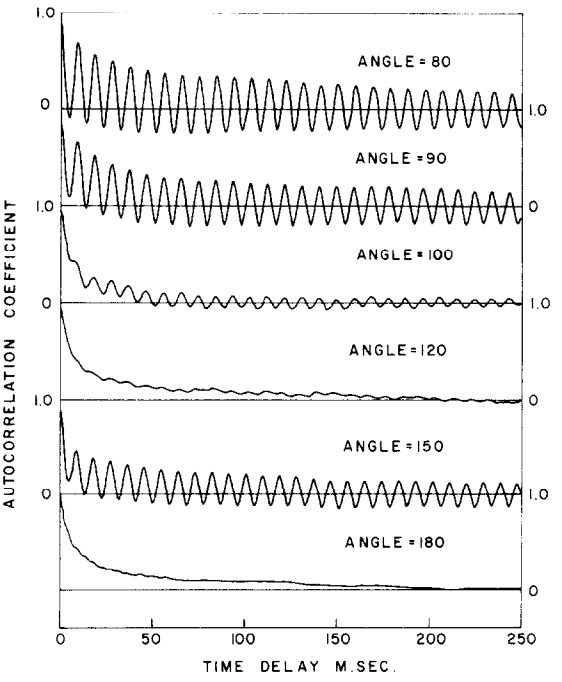

FIG. 10. Autocorrelograms of the fluctuating heat-transfer under CHF conditions, $N_{Re} = 9420$; $Tu\% = 5{\cdot}43$.

The above features of the autocorrelograms were consistent at different Reynolds numbers but were rather sensitive to variation in the free-stream intensity of turbulence. The effect, however, is best revealed by examining the power spectral density function which supplies the same information as the autocorrelation function but in the frequency domain.

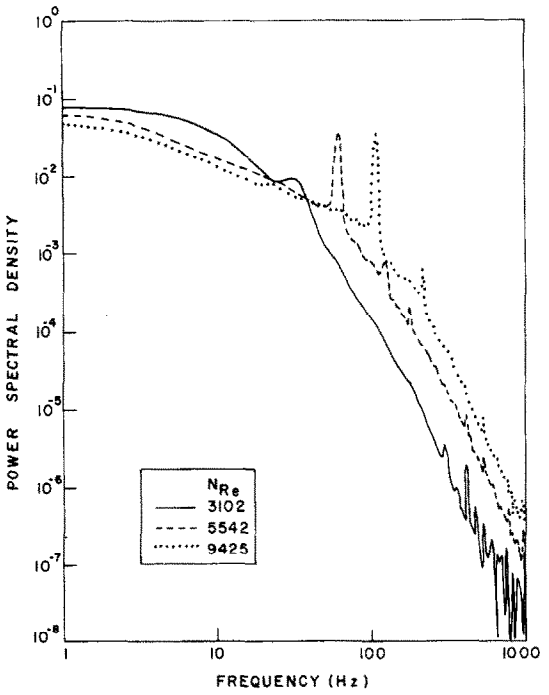

FIG. 11. Fluctuating heat-transfer spectra under CHF conditions, angle = 150°; $Tu\% = 5{\cdot}71$.

Figure 11 shows typical power spectra of the heat-transfer rate fluctuations at 150° from the fsp and different Reynolds numbers. These show distinct peaks at the shedding frequency which increases with the Reynolds number in such a way that the Strouhal number remains fairly constant at 0·21 over the Reynolds number range from 3200 to 9500. It is noticed that the high frequency content of all the spectra increases with the increase of the Reynolds number. However, in every spectrum, the rate of decay of power with frequency remains unchanged at frequencies above the shedding frequency.

It is interesting to note that the present power spectral data reveals a far more pronounced periodicity at the shedding frequency than that observed by Peterka and Richardson [19] under constant wall temperature conditions. The latter observed only a very faint periodicity while their spectra were generally "very broad and flat topped". This brings out the question whether the observed features of the local heat transfer under CHF conditions would be influenced by variations in the temperature history around the cylinder. It is with this question that the next section of this paper will be mainly concerned.

Figure 12 shows that increasing the free-stream level of turbulence, while having no effect on the shedding frequency, increases the corresponding height of the peak at the shedding frequency. The effect is best observed at 150° where the shedding frequency is most pronounced. At 180° a peak at the second harmonic is observed in the absence of the fundamental shedding frequency. In a way, this is to be expected since the rsp will be alternatively affected by the shedding from both sides of the cylinder.

A similar observation regarding the effect of free-stream turbulence on the fluctuations at the shedding frequency was reported by Liu *et al.* [20] in their measurements of the spectra of the "streaming potential fluctuations", and by Surry [21] in his spectral data of surface pressure fluctuations around a circular cylinder in a cross flow. Strangely enough, Liu *et al.* [20] also noticed a decrease of the Strouhal number below 0·21 with the increase of the free-stream intensity of turbulence. The effect seems to be related to the considerably large (L_f/d) ratio in Liu's experimental setup compared to that of the present investigation.

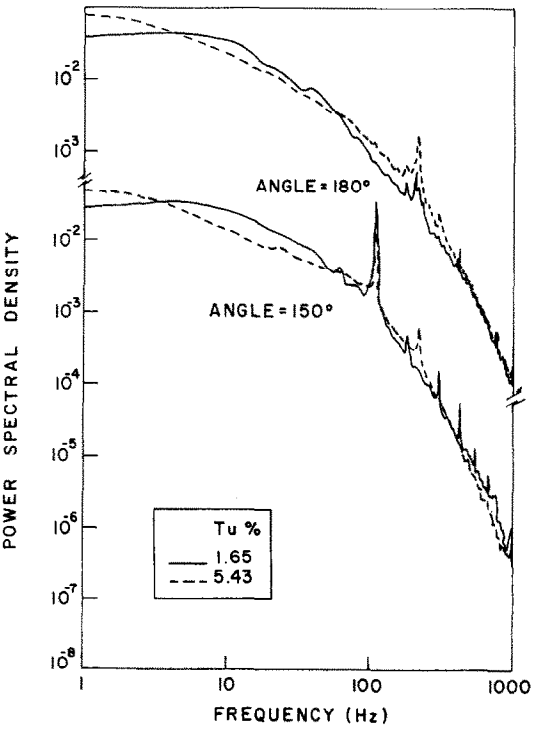

FIG. 12. Fluctuating heat-transfer spectra under CHF conditions, $N_{Re} = 9520$.

Effect of splitter plate

The splitter plate used in the present investigation was of the same length as the cylinder and 10 cm wide. It was located parallel to the axis of the cylinder with its leading edge at one and two radii from the surface of the cylinder. Experiments were carried out at three nominal Reynolds numbers under similar free-stream turbulence conditions.

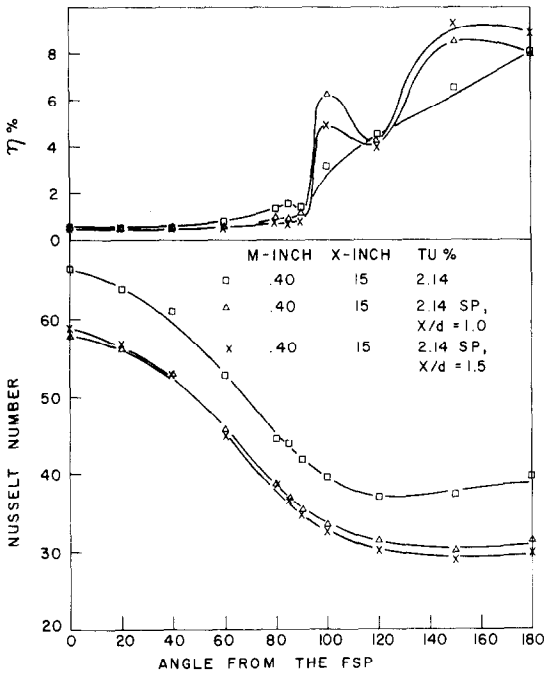

FIG. 13. Effect of the splitter plate on the local heat-transfer rate distribution under CHF conditions, $N_{Re} = 5400$.

Figure 13 shows that, in agreement with the results of Mujumdar [14], the presence of a splitter plate causes a general decrease in the local heat-transfer rate over the whole surface of the cylinder. The effect is more pronounced over the wake region and is stronger, the closer its leading edge is to the cylinder. It is also noticed that the splitter plate causes a marked increase of the intensity of heat-transfer rate fluctuations over the secondary and main vortex regions.

Typical oscillagrams of the linearized bridge voltage fluctuations over the wake region of the cylinder in the presence of the splitter plate are also shown in Fig. 8. It may be noted that the splitter plate completely suppresses all periodic components in the signal.

HEAT-TRANSFER RATE MEASUREMENTS UNDER CONSTANT WALL TEMPERATURE CONDITIONS

Although there is an abundance of litterature on heat-transfer rate measurements from cylinders under constant heat flux and constant wall temperature conditions, very little effort has been devoted to evaluate the difference between them. This is mainly because of the inherent difficulties in comparing the results of different investigators. Wind tunnel blockage, and poorly defined free-stream turbulence conditions are typical examples.

In the present investigation, a specific effort has been made to evaluate the effect of the wall temperature history on the local transfer over the wake region. Dynamic heat-transfer rate measurements were made under constant wall temperature conditions in the same wind tunnel, and using a cylinder of equal diameter to that used for the constant heat flux experiments.

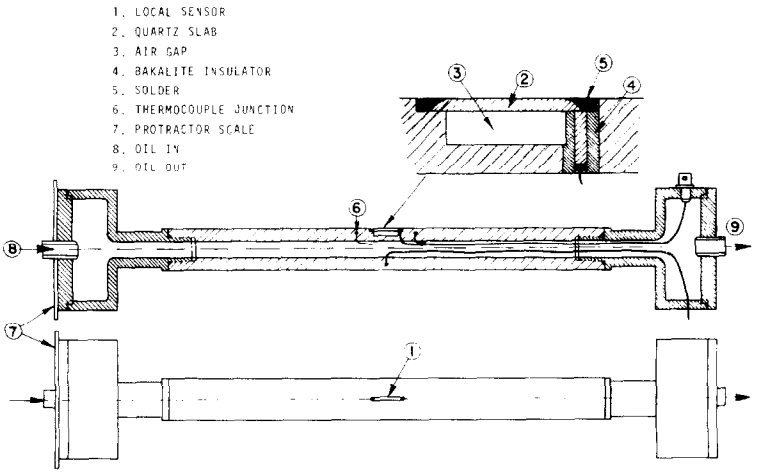

FIG. 14. Constant wall temperature test cylinder.

Experimental technique and data acquisition

The cylinder used for the local heat-transfer rate measurements under CWT (constant wall temperature) conditions is shown in Fig. 14. It was made of a heavy wall, chrome-plated, copper tube (1·87 cm O.D., 0·96 cm I.D. and 20 cm long). It was heated by internal oil circulation from a constant temperature bath. The average temperature of the cylinder was determined using five iron–constantan thermocouples embedded in its wall. The local sensor was prepared by depositing a thin film of platinum on a small quartz slab (0·13 cm wide, 1·27 cm long and 0·05 cm thick). The slab was located in a groove in the wall of the cylinder, parallel to its axis. Its azimuthal span was about 9°. Special care was taken to ensure that the edges of the slab were flush with the surface of the cylinder to within 0·0025 cm. One electrical contact from the sensor was made by a thin teflon-coated copper wire soft soldered to the platinum film and passing through the wall of the cylinder. The other contact, was made through the main body of the cylinder.

After the construction of the cylinder, the local sensor and all the thermocouples were calibrated to within $\pm 0{\cdot}25°C$ and $\pm 0{\cdot}05°C$ respectively. Due to the large size of the sensor used in this cylinder, its frequency response was relatively low. Its -3dB point was around 30 Hz. However, the attenuation was less than -6dB at 108 Hz which is the highest shedding frequency over the range of the present investigation.

The test cylinder was located in the wind tunnel by a similar arrangement as that used for the CHF cylinder described earlier. The local sensor was heated using the high sensitivity bridge of a TSI 1010A CTA unit. Its operating resistance was set such that the sensor temperature was equal to the average surface temperature of the cylinder. The circuit used was similar, although much simpler, than that used in the CHF experiment. The data analysis procedure was essentially the same.

RESULTS AND DISCUSSION

Overall heat transfer

Results of the overall heat-transfer rate measurements under constant wall temperature conditions are shown in Fig. 3 together with the corresponding constant heat flux data for comparison. It is observed that the two sets of data show essentially similar trends. However, the overall heat-transfer rate under CWT conditions was generally 10–20 per cent lower than that under CHF conditions. The difference is larger than the respective experimental error in the individual measurements and is undoubtedly caused by the differences between the temperature distributions, especially over the secondary vortex region.

A similar observation was reported by Brown, Pitts and Leppert [22] when comparing their overall transfer data from a single sphere to a fluid stream under CHF and CWT conditions. They showed that, at Reynolds numbers below 80 000 the constant heat flux data was about 10 per cent higher than the corresponding constant wall temperature data. At Reynolds numbers above 80 000, the difference was about 15 per cent.

Figure 3 also shows the effect of the intensity of turbulence on the overall Nusselt number under CWT conditions. The results are in agreement with the CHF data, with the effect of the free-stream intensity of turbulence being more pronounced at high Reynolds numbers. Moreover, there seems to be no systematic influence of the integral scale of turbulence on the overall heat-transfer rate over the range covered by the present investigation ($0{\cdot}1 < L_f/D < 0{\cdot}4$).

Local time-averaged heat transfer

Local heat-transfer rate measurements under CWT conditions were obtained at three nominal Reynolds numbers and different free-stream turbulence conditions. Typical distributions are given in Fig. 15. The complete tabulated data can be found in [9].

The distinct difference between the local heat-transfer rate distribution under CHF and CWT conditions is

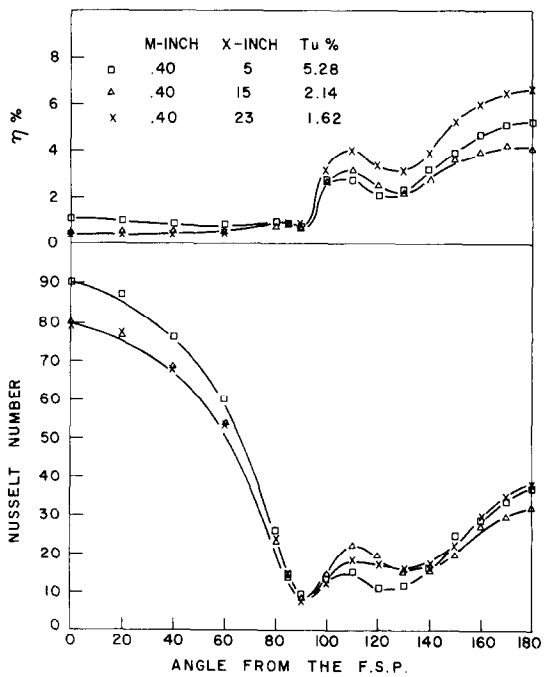

FIG. 15. Local heat-transfer rate distribution under CWT conditions, $N_{Re} = 5300$.

most remarkable. It is observed that, in agreement with the data of Galloway and Sage [10], the present measurements show a characteristic maximum in the local heat-transfer rate around 110°. The location of the minima at 90 and 130° coincide remarkably with the boundaries of the secondary vortex region as deduced earlier from the CHF data. The effect of the wall temperature history on the intensity of heat-transfer rate fluctuations over the secondary vortex region is even more pronounced than that on the time averaged heat-transfer rates. It is noticed that the value of η around 130–140° from the fsp is substantially lower under CWT than under CHF conditions.

In contrast to the secondary vortex region, the local heat-transfer rate distribution over the main vortex region showed little difference between the CWT and the CHF measurements.

Figure 16 shows that the local Nusselt number at the front and rear stagnation points have similar Reynolds number dependence under CWT conditions to that observed under CHF conditions. However, the transfer over the secondary vortex region under CWT conditions gives rise to a Reynolds number exponent of about (2/3) which is higher than that obtained under CHF conditions.

From the above it may be noted that the heat-transfer rate over the rsp is autonomous and independent of the temperature history around the cylinder.

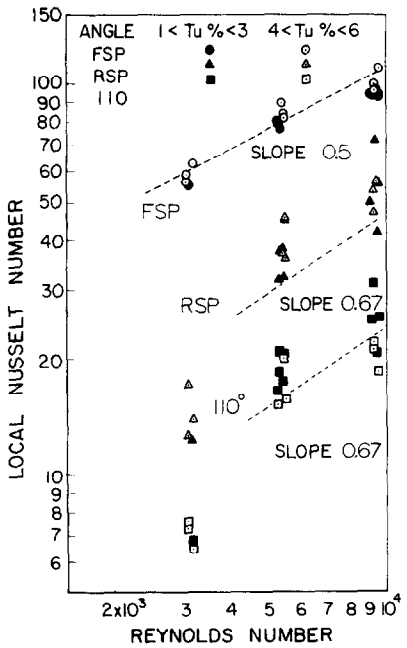

FIG. 16. Variation of the local Nusselt number with the Reynolds number under CWT conditions.

However, it can hardly be over-emphasized that one must distinguish between the transfer characteristics over the main vortex region and those over the secondary vortex region. The latter is very sensitive to variations in the temperature history around the cylinder.

Dynamic aspects of the heat transfer

In agreement with the CHF data, the signals over the secondary vortex region showed distinct spikes, while around the rsp they were more random in nature. However, there was no detectable signs of periodicity in any of the signals over the whole wake region.

Figure 17 shows typical PDF of the fluctuating heat-transfer rate over the wake region. These confirmed the observations made earlier under CHF conditions, and indicates that the temperature history around the cylinder has no effect on the fluctuating heat transfer characteristics in the amplitude domain. The latter is solely a function of the location within the wake region.

Typical autocorrelograms of the local heat-transfer rate fluctuations at different angles within the wake region are shown in Fig. 18. It is observed that at 150° there is a faint periodicity at the shedding frequency. However, at all other angles within the wake region, the only detectable periodicity is that of a 60 Hz instrument noise which was also observed even in the presence of a splitter plate.

Figure 19 shows typical power spectra of the fluctuating heat-transfer rate at 150° from the fsp under different free-stream turbulence conditions. It may be noted that, in agreement with earlier measurements, increasing the free-stream level of turbulence had no effect on the frequency of vortex shedding, but amplified the fluctuations at that frequency.

It should be pointed out that the observed lack of periodicity at the shedding frequency over the wake region seems to be characteristic of the transfer under CWT conditions. This does not imply any change in the flow pattern around the cylinder, but rather, a fluctuation in the temperature field which is out of phase with the velocity fluctuations, and is high in comparison to the local temperature difference between the surface of the cylinder and the air in its immediate vicinity.

CONCLUSIONS

From the above it is clear that any realistic correlation of the heat-transfer rate over the wake region is best to separate contributions of the secondary and the main vortex regions as follows:

$$(N_{Nu})_{\text{wake}} = aN_{Re}^{n} + bN_{Re}^{m} \tag{7}$$

where the first term on the r.h.s. represents the contribution of the secondary vortex region, while the

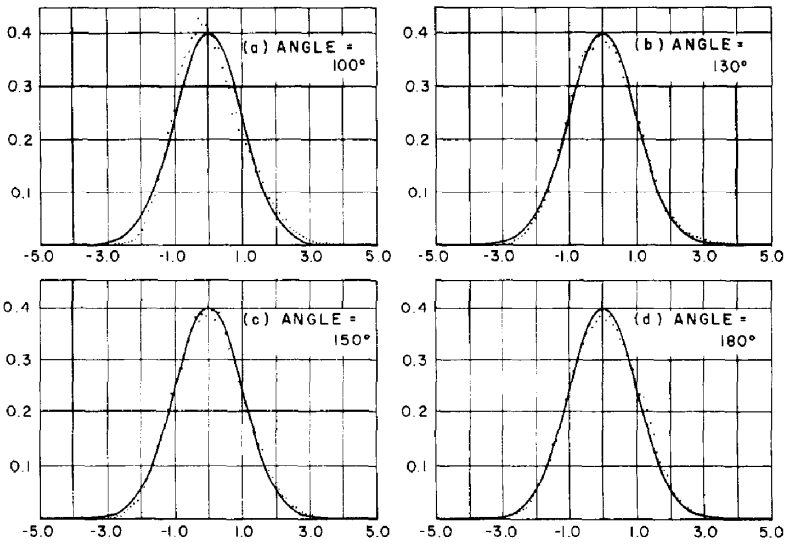

FIG. 17. Probability density function of the heat-transfer rate fluctuations under CWT conditions, $N_{Re} = 5400$; $Tu\% = 1{\cdot}62$.

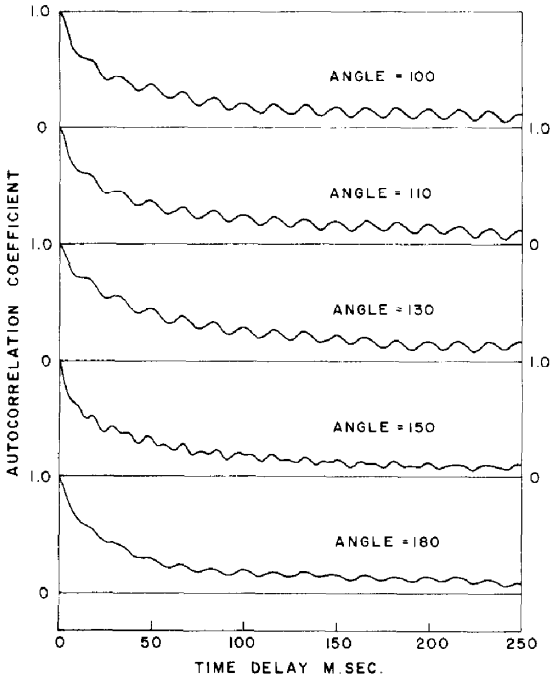

FIG. 18. Autocorrelograms of the fluctuating heat-transfer under CWT conditions, $N_{Re} = 9300$; $Tu\% = 5{\cdot}43$.

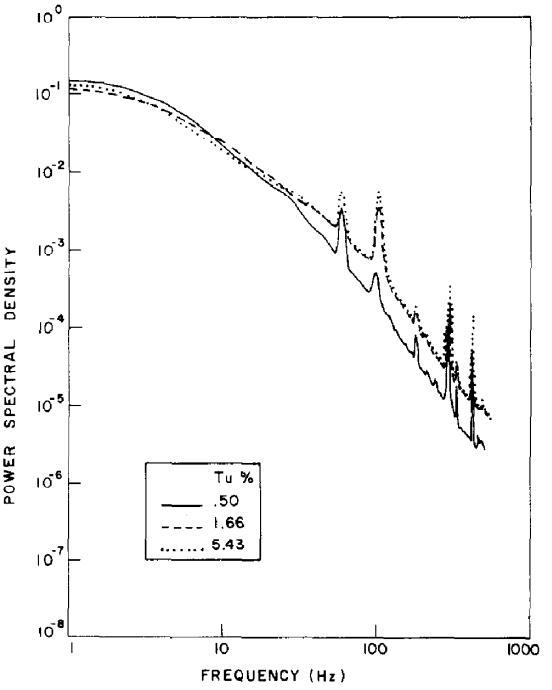

FIG. 19. Fluctuating heat-transfer spectra under CWT conditions, $N_{Re} = 9500$; angle = 150°.

second term the main vortex region. Obviously, different values of a and n will be needed to correlate data obtained under constant heat flux and constant wall temperature conditions. As to the coefficient b it will mostly be a function of the free-stream turbulence conditions. The value of the Reynolds number exponent, m, could be taken as 0·67 based on the analysis by Richardson [2] for the rsp.

The following conclusions can also be made from the present investigation.

1. The separation point of the boundary-layer oscillates at the shedding frequency between 80 and 90° from the fsp.

2. The enhancement effect of free-stream turbulence on the local time-averaged heat transfer rate over the boundary-layer region is the result of boundary-layer penetration by free-stream vortices which increase the "apparent level of turbulence" in the laminar boundary layer.

3. The overall heat-transfer rate under constant heat flux conditions is about 10–20 per cent higher than that under constant wall temperature conditions.

REFERENCES

1. W. J. M. Douglas and S. E. Churchill, Recorrelation of data for convective heat transfer between gases and single cylinders with large temperature differences, *Chem. Engng Prog. Symp. Ser.* No. 18 **52**, 23 (1956).
2. P. C. Richardson, Heat and mass transfer in turbulent separated flows, *Chem. Engng Sci.* **18**, 149 (1963).
3. S. W. Churchill and J. C. Brier, Convective heat transfer from a gas stream at high temperature to a circular cylinder normal to the flow, *Chem. Engng Prog. Symp. Ser.* No. 17 **51**, 57 (1955).
4. S. Goldstein, *Modern Developments in Fluid Dynamics*. Clarendon Press, Oxford (1938).
5. J. S. Son and T. J. Hanratty, Velocity gradients at the wall for flow around a cylinder at Reynolds numbers from 5×10^3 to 10^5, *J. Fluid Mech.* **35**, 353 (1969).
6. F. B. Hanson and P. D. Richardson, The near-wake of a circular cylinder in cross flow, *J. Basic Engng* **90**, 476 (1968).
7. M. S. Bloor, The transition to turbulence in the wake of a circular cylinder, *J. Fluid Mech.* **19**, 290 (1964).
8. P. E. Nielsen and C. G. Rasmussen, Measurements of amplitude and phase characteristics, DISA Information, No. 4, 17 (1966).
9. M. I. Boulos, Dynamics of heat transfer from cylinders in a turbulent air stream, Ph.D. Thesis, University of Waterloo (1972).
10. T. R. Galloway and B. H. Sage, Local and macroscopic transport from a 1·5 inch cylinder in a turbulent air stream, *A.I.Ch.E. Jl* **13**, 563 (1967).
11. W. H. McAdams, *Heat Transmission*, 3rd Edn. McGraw-Hill, New York (1954).
12. H. Matsui, N. Nishiwaki, M. Hirata and K. Torii, Heat transfer phenomena in wake flow of cylinders, presented at the Fourth International Heat Transfer Conference, Paris, Vol. 2, FC 5.9 (1970).
13. E. P. Dyban and E. Ya Epick, Some heat transfer features in the air flows of intensified turbulence, presented at the Fourth International Heat Transfer Conference, Paris, Vol. 2, FC 5.7 (1970).
14. A. S. Mujumdar, The effect of free-stream turbulence on heat transfer from cylinders in cross flow, Ph.D. Thesis, McGill University (1971).
15. H. C. Perkins, Jr and G. Leppert, Local heat transfer coefficients on a uniformly heated cylinder, *Int. J. Heat Mass Transfer* **7**, 143 (1964).
16. J. H. Gerrard, The mechanism of the formation region of vortices behind bluff bodies, *J. Fluid Mech.* **35**, 401 (1966).
17. A. S. Mujumdar and W. J. M. Douglas, Autocorrelation measurements in the near wake of square cylinders in turbulent free-streams, *Physics Fluids* **13**, 1635 (1970).
18. J. H. Gerrard, The three-dimensional structure of the wake of a circular cylinder, *J. Fluid Mech.* **25**, 143 (1966).
19. J. A. Peterka and P. D. Richardson, Effect of sound on separated flows, *J. Fluid Mech.* **37**, 265 (1969).
20. H. Liu, G. Binder and J. E. Cermak, Streaming potential fluctuation around a cylinder in water, *I/EC Fundamentals* **9**, 211 (1970).
21. D. Surry, Some effect of intense turbulence on the aerodynamics of a circular cylinder at subcritical Reynolds number, *J. Fluid Mech.* **52**, 543 (1972).
22. W. S. Brown, C. C. Pitts and G. Leppert, Forced convective heat transfer from a uniformly heated sphere, *J. Heat Transfer* **84**, 133 (1962).

DYNAMIQUE DU TRANSFERT DE CHALEUR PAR LES CYLINDRES DANS UN ECOULEMENT TURBULENT D'AIR

Résumé—On a étudié la dynamique du transfert de chaleur par un cylindre circulaire dans un courant d'air turbulent en considérant plus particulièrement la région de sillage.

Les résultats, obtenus pour un domaine de nombre de Reynolds compris entre 3000 et 9000, indiquent clairement que le sillage comprend deux régions distinctes: les régions principale et secondaire tourbillonnaires. La première s'étend entre 85° et 130–150° à partir du point d'arrêt amont, tandis que la seconde couvre la surface restante du sillage. Ces deux régions réagissent différemment aux variations dans l'écoulement potentiel.

DIE DYNAMIK DES WÄRMEÜBERGANGS VON ZYLINDERN IN TURBULENTER LUFTSTRÖMUNG

Zusammenfassung—Es wurde die Dynamik des Wärmeübergangs von Kreiszylindern in turbulenter Luftströmung untersucht, wobei die Vorgänge im Totwasserbereich spezielle Beachtung fanden.

Die im Bereich von $3000 < Re < 9000$ gewonnenen Ergebnisse zeigen deutlich, daß der Totwasserbereich

aus einer Hauptwirbelzone und einer Sekundärwirbelzone besteht. Die Sekundärwirbelzone liegt im Bereich zwischen Umfangswinkeln von 85° bis 130°–150° vom Staupunkt, die Hauptwirbelzone nimmt den restlichen Totwasserbereich ein. Es wird gezeigt, daß beide Zonen unterschiedlich auf Veränderungen der Anströmbedingungen reagieren.

ТЕПЛООБМЕН ЦИЛИНДРОВ В ТУРБУЛЕНТНОМ ПОТОКЕ ВОЗДУХА

Аннотация — Проведено исследование переноса тепла от кругового цилиндра в турбулентном потоке воздуха, причем, основное внимание уделено области следа.

Результаты, полученные в диапазоне чисел Рейнольдса от 3000 до 9000, ясно показывают, что след состоит из двух четко выраженных вихревых областей: вторичной и основной. Первая область лежит между 85° и 130–150° от передней критической точки, а вторая занимает остальную часть следа. Показано, что эти две области различно реагируют на изменения условий в свободном потоке.